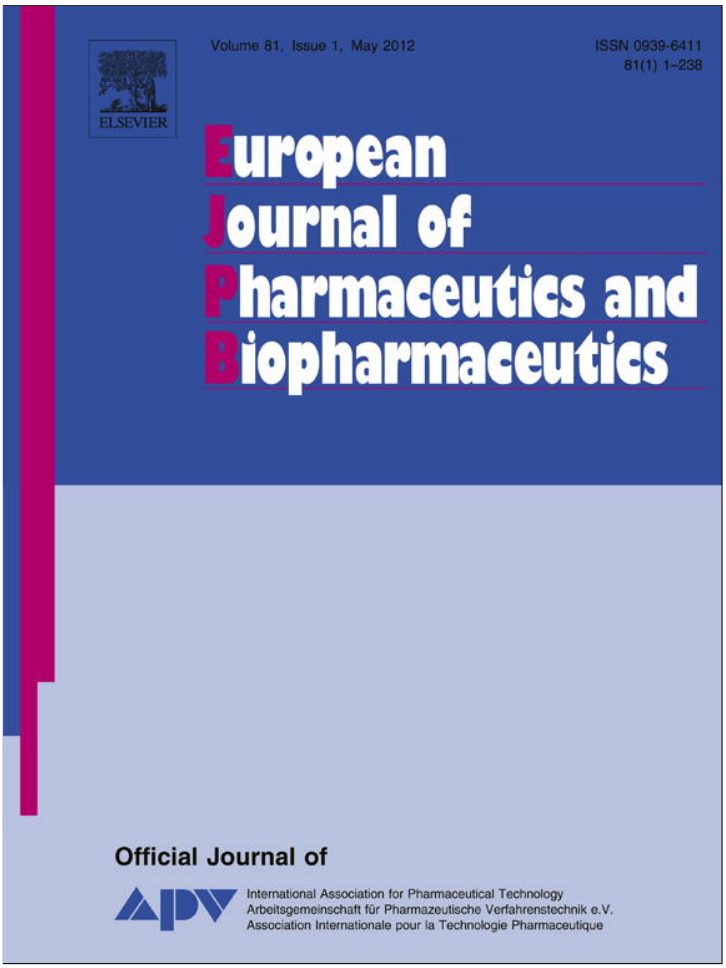

European Journal of Pharmaceutics and Biopharmaceutics 81 (2012) 91–101

Contents lists available at SciVerse ScienceDirect

European Journal of Pharmaceutics and Biopharmaceutics

journal homepage: www.elsevier.com/locate/ejpb

Research paper

Layered inorganic nanocomposites: A promising carrier for 5-fluorouracil (5-FU)

Bhavesh D. Kevadiya [a,d,1], Tapan A. Patel [b,2], Devendrasinh D. Jhala [b,2], Rahul P. Thumbar [c], Harshad Brahmbhatt [a,1], Maharshi P. Pandya [d], Shalini Rajkumar [d], Prasant K. Jena [d], Ghanshyam V. Joshi [a,1], Pankaj K. Gadhia [c,3], C.B. Tripathi [e,4], Hari C. Bajaj [a,*]

[a] Discipline of Inorganic Materials and Catalysis, Central Salt and Marine Chemicals Research Institute, Council of Scientific and Industrial Research (CSIR), Bhavnagar, Gujarat, India
[b] Department of Zoology, University School of Sciences, Gujarat University, Ahmedabad, India
[c] Department of Biosciences, Veer Narmad South Gujarat University, Surat, Gujarat, India
[d] Institute of Science, Nirma University, Ahmedabad, Gujarat, India
[e] Department of Pharmacology, Government Medical College, Bhavnagar, Gujarat, India

ARTICLE INFO

Article history:
Received 6 October 2011
Accepted in revised form 9 January 2012
Available online 16 January 2012

Keywords:
Nanocomposites
Intercalation
Na^+-clay
Controlled drug release
Genotoxicity

ABSTRACT

We report here the intercalation of 5-fluorouracil (5-FU), an anticancer drug in interlayer gallery of Na^+ clay (Montmorillonite, MMT), with the assistance of biopolymer (chitosan, CS). The X-ray diffraction patterns, thermal and spectroscopic analyses indicated the drug intercalation into the clay interlayer space in support of CS and stabilized in the longitudinal monolayer by electrostatic interaction. *In vitro* drug release showed controlled release pattern. The genotoxic effect of drug was *in vitro* evaluated in human lymphocyte cell culture by comet assay, and results indicated significant reduction in DNA damage when drug was intercalated with clay and formulated in composites. The results of *in vitro* cell viability assay in cancer cells pointed at decreased toxicity of drug when encapsulated in Na^+-clay plates than the pristine drug. In vivo pharmacokinetics, biodistribution, hepatotoxicity markers, e.g., SGPT and SGOT, and liver/testicular histology in rats showed plasma/tissue drug levels were within therapeutic window as compared to pristine drug. Therefore, drug–clay hybrid and composites can be of considerable value in chemotherapy of cancer with reduced side effects.

1. Introduction

5-Fluorouracil (5-FU) is an effectual chemotherapy option available for the treatment for colorectal cancer, stomach cancer, breast cancer, brain tumor, liver cancer, pancreatic cancers and lung cancer [1–9]. It is a pyrimidine analog that inhibits the biosynthesis of deoxyribonucleotides for DNA replication by inhibiting thymidylate synthase activity, leading to thymidine depletion, incorporation of deoxyuridine triphosphate into DNA and cell death [10,11]. An additional mechanism of cytotoxicity is the incorporation of uridine triphosphate into RNA, which disrupts RNA synthesis and processing [12]. However, 5-FU has limitations such as short biological half-life due to rapid metabolism, incomplete and non-uniform oral absorption due to metabolism by dihydropyrimidine dehydrogenase [13–16], toxic side effects on bone marrow and gastrointestinal tract and non-selective action against healthy cells [17]. For successful cancer treatment, overcoming the toxic side effects on bone marrow or GI track is enormously required, which might possibly be achieved by the control release of the drug by intercalation of drug in the clay interlayer and biopolymeric systems. Recently, various inorganic hybrid composites have emerged as an imperative class of drug delivery systems in biomaterial field. Among them, layered silicate materials, e.g., montmorillonite (MMT), have attracted a great deal of attention due to their ability to release drugs in a controlled manner [18,19], mucoadhesiveness and potent detoxification eventually leading to high efficacy of drugs. It also has capability to adsorb dietary toxins, microbial toxins associated with gastrointestinal turbulences, hydrogen ions in acidosis and metabolic toxins such as steroidal metabolites associated with pregnancy [19]. Na^+-clay has also been proved to be non-toxic by hematological, biochemical and histopathological studies in rat models [20].

In this study, we employed 5-FU intercalation in Na^+-clay interlayer gallery with the assistance of CS to overcome drug toxicity and to enhance bioavailability of the drug. The 5-FU/CS-MMT

* Corresponding author. Discipline of Inorganic Materials and Catalysis, Central Salt and Marine Chemicals Research Institute, Council of Scientific and Industrial Research (CSIR), Gijubhai Badheka Marg, Bhavnagar 364 021, Gujarat, India. Tel.: +91 278 2471793; fax: +91 278 2567562.
E-mail addresses: zooldeptgu@satyam.net.in (D.D. Jhala), shalini.rjk@nirmauni.ac.in (S. Rajkumar), pankajkgadhia@gmail.com (P.K. Gadhia), cbtripathi@yahoo.co.in (C.B. Tripathi), hcbajaj@csmcri.org (H.C. Bajaj).
[1] Tel.: +91 278 2471793; fax: +91 278 2567562.
[2] Tel.: +91 7926302362; fax: +91 7926303196.
[3] Tel.: +91 261 2227141.
[4] Tel.: +91 278 2510236; fax: +91 278 2422011.

0939-6411/$ - see front matter © 2012 Elsevier B.V. All rights reserved.
doi:10.1016/j.ejpb.2012.01.004

composites were prepared under optimal reaction conditions by ion-exchange method and characterized. The 5-FU/CS-MMT composites were evaluated for *in vitro* release characteristics, release kinetics and computational model fitting for the evaluation of drug/biopolymer–clay interactions. *In vitro* genotoxic assessments of drug were measured by degree of DNA (%) damage and *in vitro* cancer cell viability assay. Pharmacokinetics, biodistribution and histopathological study in rats were also evaluated after oral administration.

2. Materials and methods

2.1. Starting materials and reagents

For the present study, Chitosan (CS) (Viscosity: 200 cps in 1% glacial acetic acid, deacetylation degree (DD) 80%, Avg. Molecular weight: 8400), cellulose acetate dialysis tube (Cutoff molecular weight at −7000), trizma base, ethidium bromide and Lectin/PHA-P were purchased from Sigma–Aldrich, USA. 5-Fluorouracil (5-FU) was obtained from SISCO Research Laboratory Pvt. Ltd., India. Triton X 100, low melting point agarose (LMP), normal melting point agarose (NMP), RPMI-1640 (Roswell Park Memorial Institute 1640), trypan-blue, MTT (3-(4,5-dimethylthiazole-2-yl)-2,5-diphenyl tetrazolium bromide), 0.25% trypsin and 0.02% EDTA mixture, streptomycin, penicillin, amphotericin and DMSO were procured from Himedia Laboratory, Mumbai, India. FBS (fetal bovine serum) (GIBCO) was procured from Invitrogen, UK. All the other reagents were of HPLC grade and were used as received. Millipore water was processed by Milli-Q plus System (Millipore Corporation, USA).

2.2. Preparation of clay–drug composites

2.2.1. Purification of MMT

The MMT rich bentonite was collected from Akli mines, Barmer district, Rajasthan, India and purified as reported earlier [18]. In brief, 300 g of raw bentonite lumps were dispersed in 3 l of 0.1 M NaCl solution and stirred for 12 h to get Na^+–MMT. The dispersion was reacted three times with 0.1 M NaCl solution, centrifuged and washed with de-ionized water until free of chloride. The purified MMT was obtained by dispersing 150 g of Na–MMT in 10 l deionized water and collecting the supernatant dispersion of particles <2 μm after the pre-calculated time (10 h) and height (15 cm) at 30 °C. The MMT dispersion was dried at 90–100 °C and ground to pass through the 200 mesh sieve (ASTM).

2.2.2. The drug–clay hybrid intercalation

The clay–drug composite was prepared by the reported procedure [21]. In brief, 100 ml aqueous solution of 5-FU (200 mg) was treated with 100 mg of MMT under continuous shaking (Julabo shaking water bath, SW23) for 5 h at 80 °C. The mixture was centrifuged, and the concentration of free drug in the filtrate was quantified by UV–visible spectroscopy.

2.3. Preparation of the chitosan/layered silicate composites

For the preparation of chitosan/layered silicate composites, MMT (2 g) was suspended in 100 ml of Milli-Q water for 24 h, followed by 1 h sonication. The 1% (w/v) CS was prepared by dispersing it in 1% (v/v) glacial acetic acid. The pH of suspension was adjusted to 5.5 and added drop wise with a peristaltic pump to the MMT suspension. The suspension was stirred (800 rpm) at 50 °C for 48 h. The composites were collected by centrifuging the suspension at 10,000 rpm for 30 min, 20 °C (Kubota-6500, Kubota Corporation, Japan) and re-dispersing the composite pellets in Milli-Q water. This procedure was repeated till it was free from acetate. The pellet was dried at 60 °C and subsequently pulverized to 200 mesh. The CS:MMT(w/w) ratio of 0.5:1, 1:1, 2:1, 3:1, 4:1 and 5:1 were examined for drug loading/ release. Finally, the CS:MMT weight ratio of 4:1 was selected for further studies based on XRD, FT-IR and thermal analysis. This sample was designated as CS-MMT composites.

2.4. Influence of physicochemical parameters on drug–clay composites

2.4.1. Influence of pH

The CS solutions from stock solution were slowly added to the flasks containing 5-FU solution. The 5-FU/CS solutions were reacted with 2% (w/v) of MMT suspension in the pH range from 2 to 6. All experiments were performed by shaking the mixture at 50 °C for 48 h. The suspensions of free drug were centrifuged, washed and quantified in filtrate spectrophotometrically.

2.4.2. Effect of Initial drug concentration

Forty milliliters of CS (1% w/v) solution from stock solution were gradually mixed with different amount of 5-FU (10–200 mg). The 5-FU/CS solutions were treated with 5 ml (2% w/v) of MMT suspension, while being sonicated, the volume and pH (5.5) of the solutions were adjusted with continuous shaking at 50 °C for 48 h. The suspensions were centrifuged, washed and quantified.

2.5. Characterization

X-ray diffraction (XRD) analysis was carried out on Phillips powder diffractometer X' Pert MPD using PW3123/00 curved Ni-filtered Cu Kα radiation with a scanning of 0.3°/min 2θ range of 2–10°. Fourier transform infrared spectra (FT-IR) were recorded on Perkin–Elmer, GX-FTIR as KBr pellet over the wavelength range 4000–400 cm^{-1}. Thermo gravimetric analysis (TGA) was carried out within 50–800 °C at the heating rate of 10 °C/min under nitrogen flow (20 ml/min) using TGA/SDTA 851e, Mettler-Toledo, Switzerland. The parameters of differential scanning calorimetric (DSC) were measured in the range of 30–400 °C at the rate of 10 °C/min under nitrogen flow of 10 ml/min (Mettler-Toledo, DSC-822e, Switzerland). The UV–visible absorbance of drug solutions were measured at λ_{max} = 264 nm using UV–visible spectrophotometer UV2550 (Shimadzu, Japan), equipped with a quartz cell having a path length of 1 cm.

2.6. In vitro drug release

In vitro release of drug was carried out in USP eight stage dissolution test apparatus (Veego, Mumbai, India) by dialysis bag technique [18] using buffer solutions of pH 1.2 and pH 7.4 as dissolution medium. In brief, precise amounts of 5-FU, 5-FU-MMT and 5-FU/CS-MMT dispersed in 5 ml release medium were placed into an activated cellulose dialysis tube, which was placed in the basket and immersed in 500 ml release medium. The temperature was maintained at 37 ± 0.5 °C with the rotation frequency maintained at 100 rpm. Aliquots (5 ml) were withdrawn at the predetermined time intervals and refilled immediately with the same volume of the fresh medium and the drug release quantified by UV absorption.

2.7. Drug release kinetics

In order to understand the drug release mechanisms, the results obtained were fitted in Higuchi and Korsmeyer–Peppas kinetic models. The Higuchi model describes the release of drugs as square root of time based on Fickian diffusion (Eq. (1)).

$$Q = k_H t^{1/2} \quad (1)$$

k_H is the constant reflecting the design variables of the system.

Korsmeyer et al. [22] had derived a relationship for drug release kinetics (Eq. (2)) which is as follows:

$$M_t/M_\infty = Kt^n \quad (2)$$

where M_t/M_∞ is the fraction of drug released at time t, K is the rate constant and n is the diffusion exponent identifying the release mechanism of drug. Values of "n" between 0.5 and 1.0 indicate anomalous transport kinetics, 0.5 indicates the purely diffusion controlled mechanism (Fickian diffusion). The slighter values of $n < 0.5$ may be due to drug diffusion partially through an enlarged matrix or water filled pores in the formulations [18].

2.8. In vitro genotoxicity assessments

2.8.1. Lymphocyte cell culture and exposure to drug/composites

The normal human peripheral blood lymphocyte culture was used for single cell gel electrophoresis assay for the evaluation of DNA damage by actions of pristine 5-FU, 5-FU-MMT hybrid and composites. DNA lesions were expressed as % DNA damage in comet tail. For lymphocyte culture, 5 ml of whole blood from a non-smoker healthy volunteer was collected in heparinized vial by venipuncture method. Lymphocyte culture was seeded in autoclaved micro-centrifuge tubes (2 ml) as described by Hungerford [23] with slight modifications. In brief, 100 µl of whole blood was re-suspended in micro-centrifuge tubes containing 1.5 ml RPMI 1640 and 20 µl PHA-P and transferred in CO_2 incubator (Heracell 150i, Thermo Fisher Scientific) at 37 °C temperature and 5% CO_2 for incubation. Cultures were set in five groups with G_1 as untreated control group, G_2 as drug carrier control (CS-MMT, 30 ng), G_3 as positive control (5-FU, 6 ng), G_4 as 5-FU-MMT and G_5 with 5FU/CS-MMT. The G_4 and G_5 were further ramified by 10 cultures in each set. Each culture was treated with 5-FU-MMT (30 ng) and 5-FU/CS-MMT (11.5 ng), respectively, in series at 60th h after seeding. The first culture was harvested after 1 h of treatment and then sustained with the next culture at time interval of 1 h, thus exposing first culture for 1 h and the last culture for 10 h. The time duration was determined considering the drug liberated from hybrid and composites in the cell culture medium.

2.8.2. Single cell gel electrophoresis (comet assay)

The genotoxicity of drug containing composites was determined by calculating DNA damage using comet assay, based on the measurement of DNA migration under electrophoresis as per slightly modified technique given by Singh et al. [24]. In brief, 180 µl of 1% Normal melting point (LMP) agarose (NMP) was gelled on fully frosted slide (75 mm X 25 mm), and 100 µl (0.5%) low melting point (LMP) agarose-containing cell suspension (20 µl) was layered on the top of the NMP agarose. After the formation of cell suspension containing layer, additional 100 µl of LMP agarose was added to fill in residual hole and to form an additional layer to increase the distance between the cells and the gel surface. After agarose gel solidification, the slides were placed in a lysis solution [2.5 M NaCl, 100 mM EDTA and 10 mM Tris–HCl (pH 10), plus 1% Triton X-100 and 10% DMSO were added just before use] for 24 h at 4 °C and incubated in alkaline electrophoresis buffer (300 mM NaOH/1 mM EDTA, pH > 13) for 40 min and electrophoresed (Midi-Submarine electrophoresis Unit-7050, Tarsons, Kolkata, India) for 35 min. After the comets were formed, the alkaline gel was neutralized by rinsing the slides with a suitable buffer (0.4 M Tris, pH 7.5) three times and the slides were stained with the fluorescent dye ethidium bromide (Et–Br). The comet images were captured using Carl zeiss Axio-Cam-MRc camera attached to Axio-Scope fluorescence microscope (Germany). The proportion of DNA damage was scrutinized by scoring 100 comets for each group (Tri-Tek Comet-Score™ V1.5 software, Germany). An intensity score from class 0 (undamaged) to class 4 (severely damaged) was assigned to each cell, based on the procedure given in Visvardis et al. [25]. Thus, the total score for the 100 comets could range from 0 to 4 as the 100 cells were observed individually in each comet assay.

2.9. Cell cultures

A549 (Human lung adenocarcinoma epithelial cell line) was obtained from National Repository of Animal Cell Culture, National Centre for Cell Sciences (NCCS), Pune, India. A549 cell line was cultured in 25 cm^2 tissue culture flasks maintained at 37 °C in a humidified environment of 5% CO_2 and was grown in RPMI-1640 with 10% FBS and 1% penicillin, streptomycin and amphotericin B (PSA) antibiotic mixture.

2.9.1. In vitro cytotoxicity assay

The viability of cancer cells treated with 5-FU, 5-FU-MMT hybrid and 5-FU/CS-MMT composites was evaluated by the MTT assay. 150 µl of A549 cells were seeded in 96-well plates (Becton Dickinson (BD), USA) at the density of 1.1×10^4 viable cells/well and incubated for 24 h to allow cell attachment. Following attachment, the medium was substituted with complete medium (150 µl/well) containing the pristine 5-FU, 5-FU-MMT hybrid and 5-FU/CS-MMT composites at equivalent drug concentrations ranging from 0.1 to 100 µg/ml for 72 h. Following treatment, the cells were then washed with PBS and incubated with 100 µl/well fresh medium containing 0.5 mg/ml MTT. The MTT containing medium was removed after incubating for 3 h in dark. The MTT formazan was dissolved in 100 µl/well DMSO, and optical density was determined at 570 nm using an ELISA plate reader (Bio-Tek, USA). Cell viability was calculated by the following equation:

$$\text{Cell viability } (\%) = (A_s/A_{control}) \times 100 \quad (3)$$

where A_s is the absorbance of the cells incubated with the 5-FU, 5-FU-MMT hybrid and 5-FU/CS-MMT composites and $A_{control}$ is the

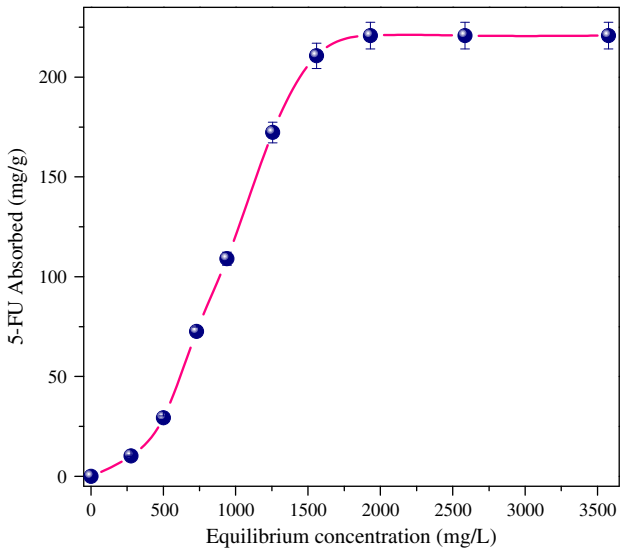

Fig. 1. The intercalation of 5-FU and CS in clay interlayer space by illustrating of equilibrium isotherm pattern and effect of concentration gradients of drug (Under optimal reaction conditions as; CS:MMT: 4:1(% w/w), pH = 5.5, temp. = 50 °C, time = 48 h), data represent mean ± SD ($n = 3$). (For the interpretation of the references to color in this figure legend, the reader is referred to the web version of this article.)

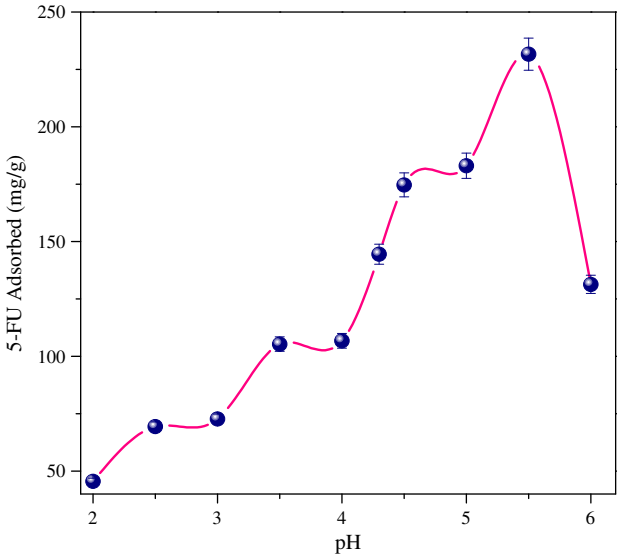

Fig. 2. Influence of pH on 5-FU and CS intercalation in clay with optimal reaction conditions as; CS: MMT: 4:1(% w/w), pH = 5.5, temperature = 50 °C, time = 48 h), Data represent mean ± SD (n = 3). (For the interpretation of the references to color in this figure legend, the reader is referred to the web version of this article.)

absorbance of the cells incubated with the culture medium only. IC_{50}, the drug concentration at which inhibition of 50% cell growth was observed when compared to control sample, was calculated by appropriate curve of cell viability data.

2.10. In vivo pharmacokinetics (PK)

2.10.1. Animals and dosing

10- to 12-week-old healthy male wistar rats weighing 200–250 g were procured from the Laboratory Animals Centre of Zydus Research Center (ZRC), Ahmedabad, India, under the Registration number 167/1999/CPCSEA from the Ministry of Social Justice and Empowerment, Government of India and Committee for the Purpose of Control and Supervision of Experiments on Animals, Chennai, India, and were maintained at the animal house of Department of Zoology, Gujarat University, Ahmedabad, India. The animal caring, handling and the protocols were approved by the Institutional Animal Ethics Committee (IAEC) of the department, Ahmedabad, India. The animals were acclimatized at temperature of 25 ± 2 °C and relative humidity of 50–60% under 12 h/12 h light/dark conditions for one week before experiments. All animals were fasted for 24 h before the studies, and water was available *ad libitum* during the course of studies. The animals were arbitrarily distributed into three groups each containing six animals. First group of animals received oral pristine 5-FU, while the second group of animals received 5-FU-MMT hybrid (suspension) and third group received 5-FU/CS-MMT composites (suspension). All the formulations were administered orally using a feeding tube attached to a hypodermic syringe at a dose of 5-FU (50 mg/kg) body weight. All animals were observed for their general condition, clinical signs and mortality. The blood samples (approximately 0.3 ml) were collected from the retro orbital plexus under mild anesthesia into the micro-centrifuge tubes containing heparin (500 units/ml blood) as an anticoagulant. The time breaks for blood collection were kept at 0 (predose), 1, 3, 6, 9, 12, 24 and 48 h after administration of the drug. Plasma samples were harvested by centrifugation (Kubota-6500, Kubota Corporation, Japan) at 10,000 rpm for 15 min at 5 °C and stored at −20 °C for HPLC analysis.

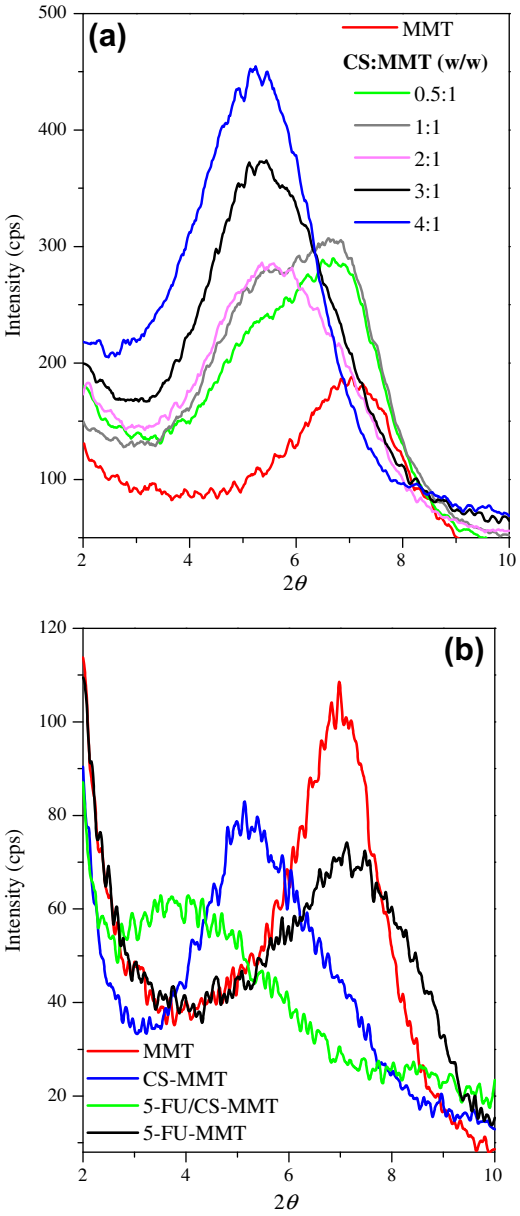

Fig. 3. XRD patterns of: (a) CS: MMT ratio optimization and (b) MMT, 5-FU-MMT, CS-MMT and 5-FU/CS-MMT. (For the interpretation of the references to color in this figure legend, the reader is referred to the web version of this article.)

2.10.2. The drug quantification by HPLC

The quantification of 5-FU from plasma was determined by using a validated HPLC method reported in literature with some modifications [26]. Briefly, subsequent to the preparation of plasma samples, analysis by high-performance liquid chromatography (HPLC) system consisting of photodiode array detector (Waters Alliance model: 2695 separation module with Waters 2996 Photodiode Array Detector, Waters Corporation, Milford, MA, USA) and a reverse-phase C18 column (Phenomenex® make Luna C18 (2) HPLC column with Length = 25 cm, ID = 4.6 mm, Particle size = 5.0 µm, Phenomenex Inc, Torrance, CA, USA) was carried out. 5-FU containing plasma samples were transferred to auto sampler vials, capped and placed in cassettes of the HPLC autosampler. Mobile phase employed for the analysis was the mixture of methanol, acetic acid and water (4:0.05:95.95, by volume). The injection volume was 5 µl, and detection wavelength (λ_{max}) for 5-FU was at 254 nm. Drug concentration in plasma was determined using the standard curve

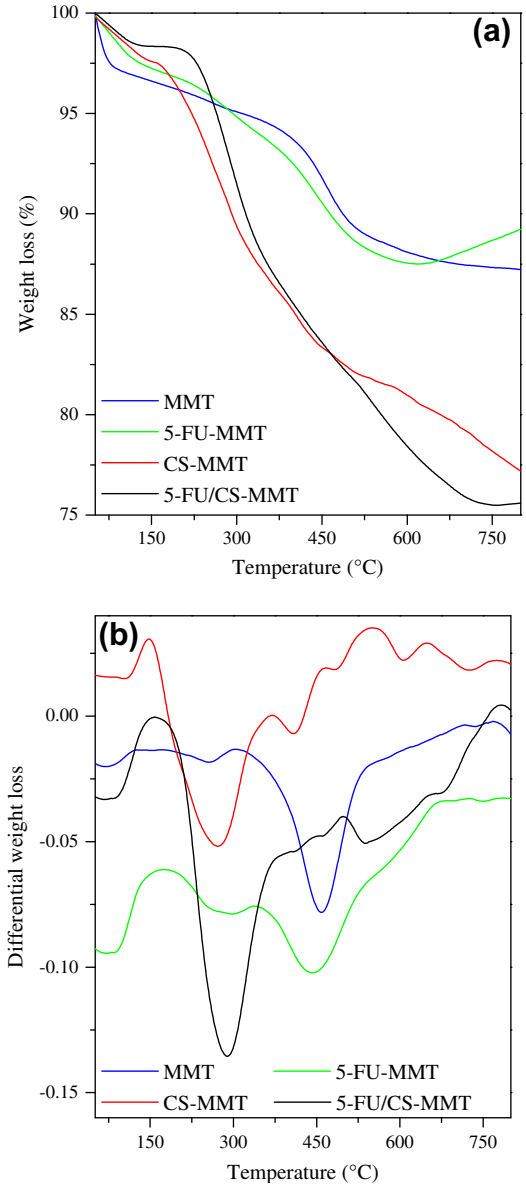

Fig. 4. (a) TGA and (b) DTA pattern. (For the interpretation of the references to color in this figure legend, the reader is referred to the web version of this article.)

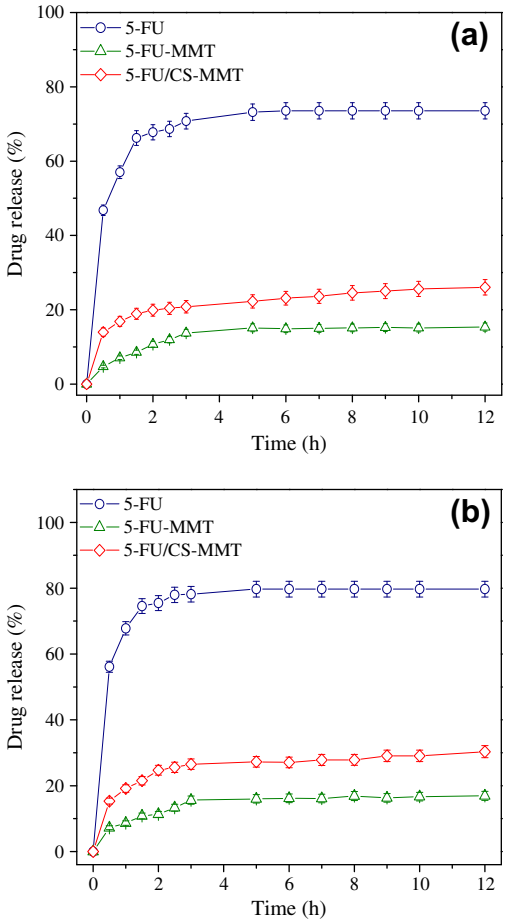

Fig. 5. *In vitro* drug release profiles of 5-FU in (a) pH 1.2 and (b) pH 7.4 at 37 ± 0.5 °C, data represent mean ± SD ($n = 3$). (For the interpretation of the references to color in this figure legend, the reader is referred to the web version of this article.)

obtained for known concentrations of 5-FU in plasma processed similarly. The curve was found to be linear with a $R^2 = 0.9994$. The pharmacokinetics parameters are total area under the curve $(AUC)_{0-\infty}$, the mean residence time (MRT), peak plasma concentration (C_{max}) and time to reach the maximum plasma concentration (T_{max}).

2.11. In vivo drug distribution in tissues, toxicity biomarkers assessment and histopathological evaluation

To evaluate the effect of the pristine 5-FU, 5-FU-MMT hybrid and 5-FU/CS-MMT composites in different tissues of rats, all animals were fasted for 24 h before the studies and water was made available *ad libitum* during the course of studies. The animals were randomly distributed into three groups each containing six animals. First group of animals received oral pristine 5-FU, while second group of animals received 5-FU-MMT hybrid (suspension) and third group received 5-FU/CS-MMT composites (suspension). All the formulations were administered orally using a feeding tube attached to a hypodermic syringe at a dose of 5-FU (50 mg/kg) body weight. All animals were observed for their general condition, clinical signs and mortality. Two animals from each group were euthanized with an intraperitoneal injection of sodium pentobarbital (120 mg/kg body weight) at 1, 3 and 12 h after drug administration. Immediately after death, carcasses were placed on ice packs and opened by bilateral thoracotomy. The heart, liver, lung, kidney, spleen and testis were collected. Tissue samples were blotted with paper towel to remove blood, rinsed in saline, blotted to remove excess fluid, weighed, cut into small pieces and then homogenized with 4 ml of 0.1 M NaOH. The homogenate was then centrifuged at 10,000 g for 30 min at 5 °C, the fatty layer was discarded and supernatants were collected for the quantification of drug by HPLC as per described above.

The drug toxicity evaluations were carried out by the collection of blood throughout the experiment from animals of each group at time intervals of 1, 3 and 12 h. The drug toxicity biomarkers, (1) ALT (Glutamate pyruvate transaminase, SGPT) and (2) AST (Serum glutamate oxaloacetate transaminase, SGOT) were estimated from rat serum by kinetic method using semiautomatic biochemistry analyzer-RA-50 (Bayer Inc., USA). A small portion of liver and testis was excised from animals of each group (12 h), fixed in 10% v/v formalin saline and processed for standard histopathological procedures. Paraffin embedded specimens were cut into 5 μm sections (Yorco Sales Pvt. Ltd., New Delhi) and stained with hematoxylin and eosin (H&E) for histopathological evaluations. The histopathological tissues sections were viewed and digitally photographed

Table 1
In vitro drug release profile and its parameters as evaluated by mathematical model.

Kinetic model	Parameter	Formulation			
		5-FU-MMT		5-FU/CS-MMT	
		pH 1.2	pH 7.4	pH 1.2	pH 7.4
Higuchi	r^2	0.9909	0.9561	0.9779	0.9813
	k_H	7.8501	7.4537	3.4888	11.252
Korsmeyer–Peppas	r^2	0.9792	0.954	0.9727	0.9915
	n	0.5360	0.3815	0.1845	0.3155
	K_{KP}	0.4601	0.5416	0.6455	0.6311

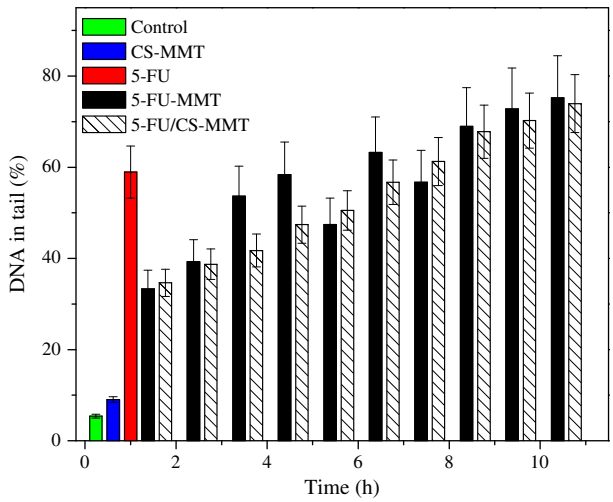

Fig. 6. Genotoxic action of drug as evaluated by the DNA damage (%) versus different exposure time to drug/formulation in lymphocyte cell culture, data represent mean ± SD ($n = 3$). (For the interpretation of the references to color in this figure legend, the reader is referred to the web version of this article.)

using a Cat-Cam 3.0 MP trinocular microscope with an attached digital 3XM picture camera (Catalyst Biotech, Mumbai, India).

2.12. Statistical analysis

All the results were expressed as mean ± standard deviation (SD). Statistical analysis was performed with Origin 8.0 (OriginLab Corporation, USA) using one-way ANOVA followed by Tukey multiple comparison test. $p < 0.05$ was considered as statistically significant difference.

3. Results and discussion

3.1. The chemistry of drug intercalation in the gallery of clay

The maximum ~8% intercalation of drug in clay has been reported at pH 11.6, 80 °C within 3 h [21]. The drug/biopolymer solution was treated with the suspension of clay under optimal pH and concentrations. Fig. 1 shows the amount of drug intercalated in clay gallery with the assistance of biopolymer (CS) at different concentrations. By increasing initial concentration of drug, improved degree of intercalation and the equilibrium were attained after intercalation of 220 mg of drug/g of clay in support of biopolymer. A significant increase in drug intercalation was observed up to pH 5.5 (Fig. 2), beyond which there was decline in drug loading. The pH 5.5 is essential for the ionization of —NH_3^+ groups from biopolymer (p*Ka* = 6.3) and ionization of drug (p*Ka* = 8.0). The drug intercalation process is primarily controlled by a cationic exchange mechanism due to the coulombic interaction between the positive —NH_3^+ group of the biopolymer and the negative charge on the clay layers [27–30].

3.2. Characterization of drug–clay hybrids

3.2.1. XRD and FT-IR analysis

The powder XRD patterns of the pristine MMT and CS:MMT composite (with varying CS-MMT ratio) are shown in Fig. 3a. Pristine MMT showed a typical XRD pattern with the basal spacing of 1.20 nm ($2\theta = 7.3°$), and intercalation of biopolymer, chitosan (CS), leads to a significant increase in interlayer space of clay. The optimized ratio of CS-MMT (4:1% w/w) showed a basal spacing of 1.79 nm ($2\theta = 4.9°$). In comparison with pristine MMT, the 2θ value of 5-FU-MMT hybrid and 5-FU/CS-MMT shifted toward lower 2θ angles at 7.1° (1.22 nm) and 3.9° (2.23 nm), respectively (Fig. 3b). Since the sheet thickness of MMT was 0.96 nm [18] and height of single chain of CS was estimated at 0.43 nm (Accelreys MS Modeling 3.2), the gallery height for 5-FU/CS-MMT composites could be estimated to be 0.41 nm. This value was slightly lower than the longitudinal molecular length (0.48 nm) and lateral length (0.45 nm) of 5-FU molecule (Fig S1, supplementary data). The enlarged basal spacing may be due to the uptake of two CS chains ($0.43 \times 2 = 0.86$ nm) in layers and a monolayer of 5-FU molecules in gallery of the MMT (*Sandwich model of* "*CS/5-FU/CS*"). Such a model allows enhanced electrostatic interactions between drug/biopolymer and clay layers. Thus, the drug/biopolymers were intercalated by ion-exchange reaction with Na^+ ions of the pristine clay and were preserved safely in the clay interlayer spaces by electrostatic interaction.

The FT-IR spectra of the drug/biopolymer loaded hybrid and composites were compared with that of the pristine clay and drug (Fig. S2, supplementary data). The spectrum of MMT revealed the characteristic absorption bands [18,31]. The IR spectrum of biopolymer "CS" was given the characteristic absorption bands [32]. The presence of characteristic IR bands from the CS-MMT composites confirmed the successful intercalation of biopolymer and clay. The vibration bands at 1595 cm^{-1} in CS was due to the deformation vibration of the protonated amine group, which shifted toward lower frequency of 1542 cm^{-1} in CS–MMT composites [18]. The spectra of pure drug gave peaks at 3067, 2939 and 2828 cm^{-1} attributed to both aromatic and aliphatic C—H stretching vibrations. A band at 1726 cm^{-1} represents the imide group stretching of heterocyclic ring. A sharp band at 1670 cm^{-1} is due to the tertiary amide group stretching vibrations. N—H bending vibration was observed at 1500 cm^{-1}, and a band at 1249 cm^{-1} showed C—N stretching vibrations. The band at 1426 cm^{-1} was due to

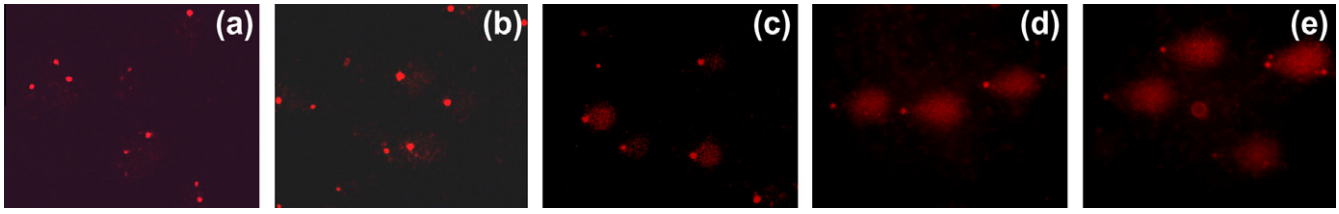

Fig. 7. Typical images (at 10× magnification) from cultured lymphocyte comet assay. After 1 h exposure time from (a) control (b) CS-MMT (c) 5-FU, and after 10 h of exposure comet from (d) 5-FU-MMT (e) 5-FU/CS-MMT. (For the interpretation of the references to color in this figure legend, the reader is referred to the web version of this article.)

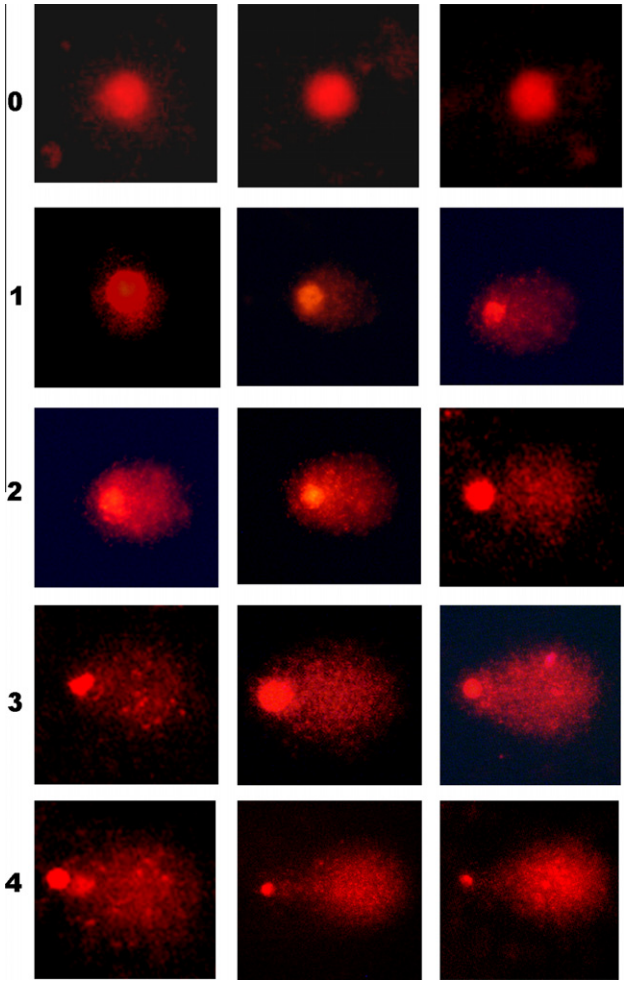

Fig. 8. The comet images of lymphocytes in (G_1) untreated control group and groups treated with (G_2) CS-MMT (G_3) 5-FU (G_4) 5-FU-MMT and (G_5) 5-FU/CS-MMT, illustrating the visual scoring classification from class 0 to 4. (For the interpretation of the references to color in this figure legend, the reader is referred to the web version of this article.)

C—H in-plane bending vibration of CF=CH group, 814 and 751 cm^{-1} due to C—H out-of-plane formation vibration of CF=CH group. On comparing the FT-IR spectrum of 5-FU-MMT or 5-FU/CS-MMT with that of MMT or CS-MMT, respectively, there were few additional bands at ~2930, 1418, 752 and 807 cm^{-1} of 5-FU, which confirmed successful intercalation of drug in clay or biopolymer/clay composites.

3.2.2. Thermal analysis

Fig. 4a illustrates the TGA pattern and Fig. 4b the DTA pattern of dried MMT and drug loaded clay hybrid or biopolymer/clay composites. The first weight loss and endothermic peak at ~100 °C in clay corresponded to the loss of adsorbed water. The weight loss (~16%) at 450 °C was due to the dehydroxylation of the MMT [18,31]. The 5-FU-MMT hybrid showed weight loss (18%) in three steps in the temperature regions of 90 °C, 280 °C and 440 °C. The first loss at 90 °C and the endothermic peak was due to free water evaporation. The second loss and endothermic peak at the temperature around 280 °C was due to onset of drug decay in clay. The final stride of weight loss was due to complete decomposition of intercalated drug in clay gallery. The weight loss temperature range between 150 °C and 600 °C in biopolymer/clay composites related to the adsorbed water molecules and showed slightly higher mass loss than clay (23%), which may be due to the high water-retention capacity of biopolymer. The content of biopolymer in the

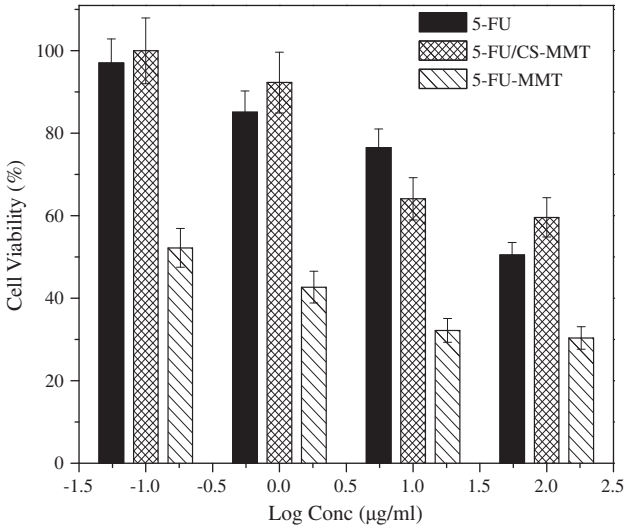

Fig. 9. *In vitro* viability of A549 (human lung adenocarcinoma epithelial cell line) cancer cells after 72 h cell culture treated with 5-FU, 5-FU-MMT and 5-FU/CS-MMT intercalated in biopolymer/MMT at 0.1–100 µg/ml of 5-FU, respectively; data represent mean ± SD (n = 6).

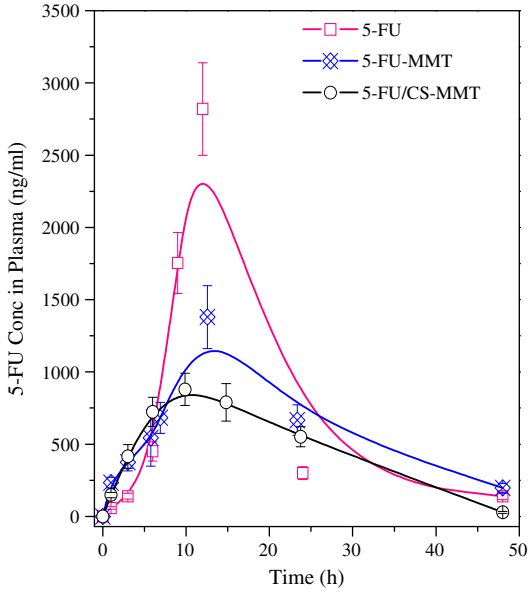

Fig. 10. Time profile of relative plasma concentrations of drug after oral administration to wistar rats when formulated in the MMT and CS-MMT as compared to pristine 5-FU, results are shown as means ± SD of 6 animals per group ($p < 0.05$). (For the interpretation of the references to color in this figure legend, the reader is referred to the web version of this article.)

biopolymer/clay composites was ~8% mass percent. The total 36% weight loss of 5-FU/CS-MMT composites in three steps was observed at 90 °C, 290 °C and 540 °C. The maximum weight loss for 5-FU/CS-MMT composites was observed at 290 °C (weight loss 20%) due to disintegration of drug. These results were in agreement with the result from XRD, revealing the intercalation of drug and biopolymer in the clay interlayer gallery.

3.2.3. Physical status of drug and biopolymer in the clay

The physical status of drug in the clay and in biopolymer/clay composites was investigated by DSC (Fig. S3, supplementary data). DSC curves of pristine clay gave a peak at 115 °C due to loss of water, whereas biopolymer/clay composites gave broad

Table 2
Pharmacokinetics of pristine 5-FU, 5-FU-MMT hybrid and 5-FU/CS-MMT in wistar rats after single oral administration of same drug dose; data represent mean ± SD, (n = 6).

PK parameter	5-FU	5-FU-MMT	5-FU/CS-MMT
C_{max} (ng/ml)	2819.78 ± 320	1358.49 ± 217	649.14 ± 109
T_{max} (h)	12	12	12
$AUC_{0-\infty}$ (ng h/ml)	37,597 ± 3985	18,575 ± 2084	13,146 ± 1262
MRT (h)	15.78 ± 1.6	37.16 ± 4.1	28.54 ± 2.6

endothermic peak at 98 °C due to the decomposition of biopolymer. The melting endothermic peak of pure drug appeared at 285 °C and second sharp exothermic peak at 350 °C due to its degradation. However, no melting peak could be detected in 5-FU-MMT and 5-FU/CS-MMT composites. The 5-FU/CS-MMT composites gave a broad peak having similar pattern as that of biopolymer, indicating that the drug/ biopolymer composites were better intercalated in clay at molecular level.

3.3. In vitro drug release study

The drug release patterns of drug from drug–clay hybrid and drug–biopolymer/clay composites in buffer solutions with the two different pH values of 1.2 and 7.4 are reported (Fig. 5a and b). The release of drug after 12 h from the clay matrix at pH 1.2 and 7.4 was ~16% and ~17%, respectively. The negative charge on clay increases with increasing pH, while drug (pKa 8.0) remains positively charged even at pH 7.4. This indicates that drug binds even more strongly to clay, and therefore it is slowly released from clay after 12 h at pH 7.4. The presence of biopolymer in the composite influences the interaction between drug and clay, which in turn accelerated the release of the drug from drug–biopolymer/clay composites. Thus, drug release was comparatively faster from the composites than from pure clay at both pH. Moreover, the presence of biopolymer in the composites is reported to result in mucoadhesion and promote bioavailability of the drug by interacting with the gastric and intestinal mucosa. Thus, increasing the biopolymer content of the biopolymer/clay composites may have increased the release rate. The release of drug from the composites could be tuned by controlling the amount of biopolymer in the composite.

3.4. Drug release kinetics

The values of correlation coefficient (r^2) and rate constants (k) for Higuchi and Korsmeyer–Peppas kinetic models are presented (Table 1). Taking into account the values of "n," drug release from drug–biopolymer/clay composites followed the controlled diffusion mechanism (Fickian diffusion) or drug diffusion partially through a swollen matrix and water filled pores in the formulations.

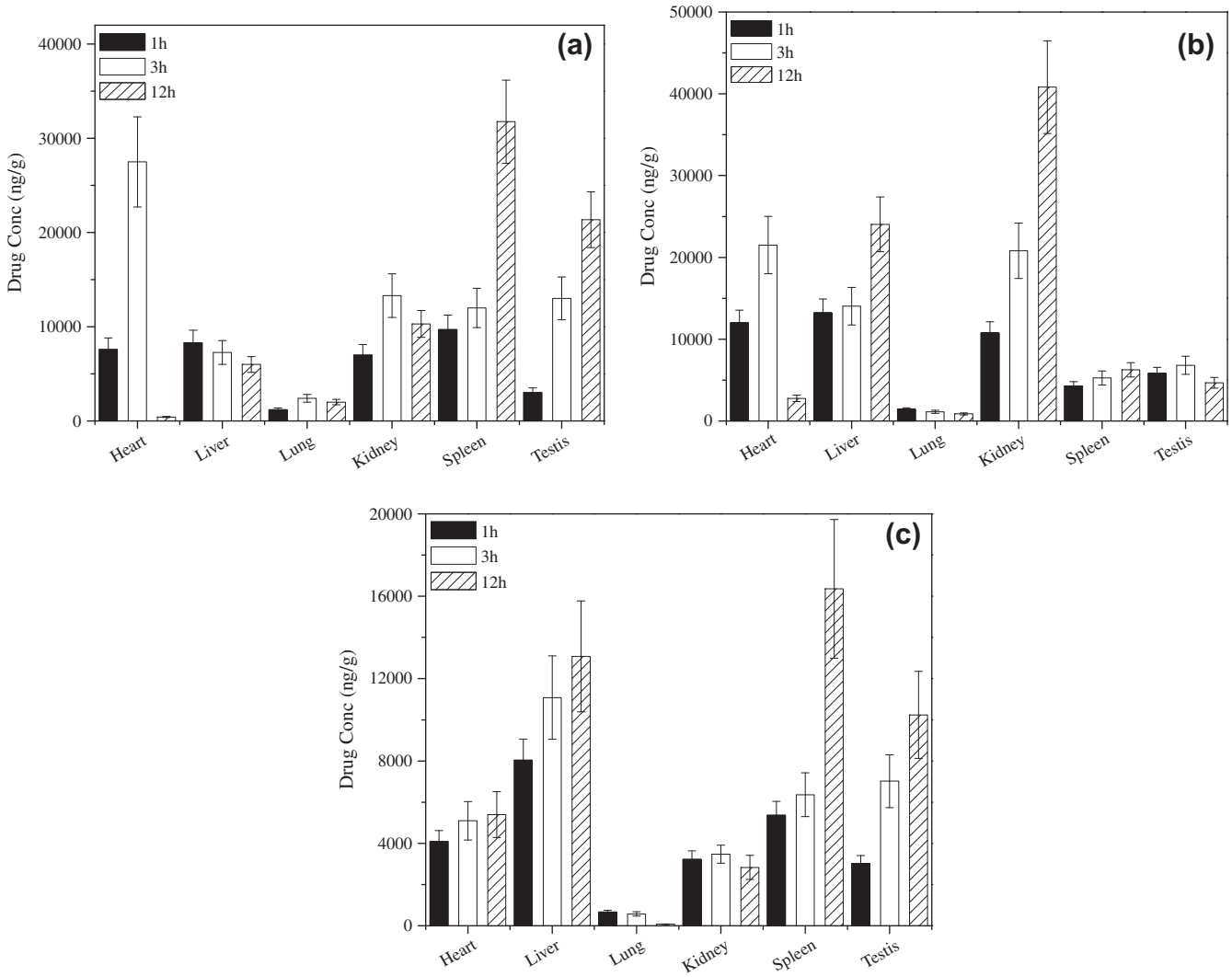

Fig. 11. Biodistribution of (a) 5-FU (b) 5-FU-MMT (c) 5-FU/CS-MMT in tissues/organs; data represent mean ± SD ($p < 0.05$).

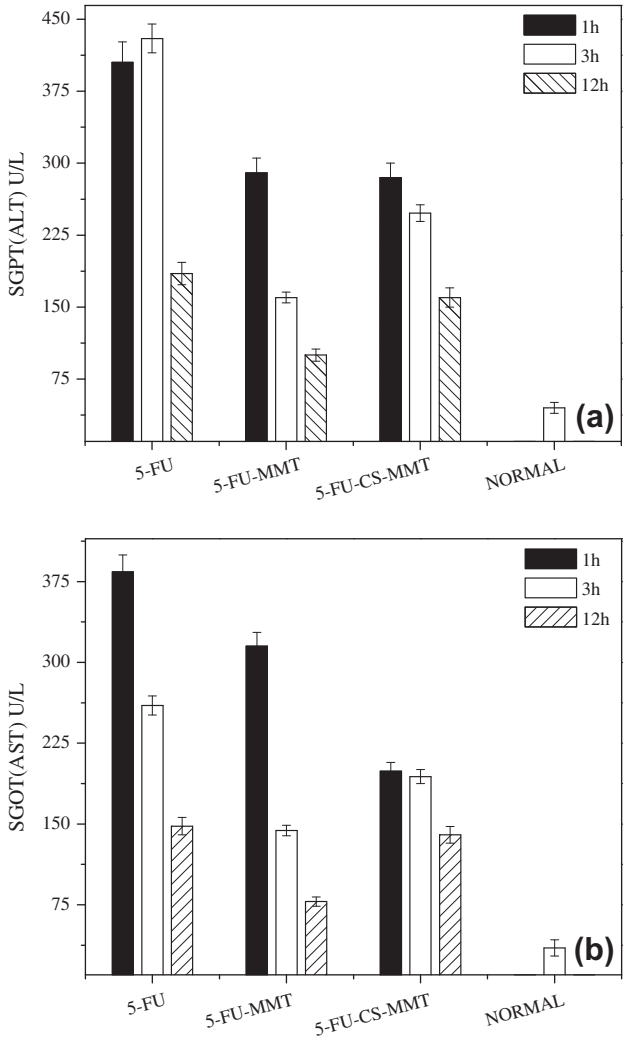

Fig. 12. (a) SGPT (ALT) and (b) SGOT (AST) levels in plasma at different time gaps after oral administration to Wistar rats when formulated in the MMT and CS-MMT as compared to pristine 5-FU; data represent mean ± SD ($n = 6$).

3.5. In vitro genotoxicity assessments

The time dependent genotoxicity of drug loaded hybrids and composites was determined up to 10 h. The results of pure drug and drug loaded hybrid/composites are shown in Fig. 6. After 1 h incubation with drug–biopolymer/clay, nearly ~35% of the measurable DNA damage had occurred this increased to ~75% in 10 h (Fig. 7d and e). The DNA damage (Fig. 7c) induced by positive (drug) and internal control (biopolymer/clay) after 1 h incubation was ~60 and ~9%, respectively (Fig. 7b). The visual score was calculated by the classification of images in five different categories (0–4 classes). The classification of percent DNA damage in tail is shown in Fig. 8, which was referred to classify observed comet tail length and tail intensity in different classes from 0 to 4. In untreated (G1) and drug carrier (G2) control groups, the majority of the cells/comets were classified into 0–2 classes, whereas in drug treated groups (G3, G4, G5), the range of comet classes was extended from 2 to 4.

3.6. In vitro cell viability with drug/biopolymer/clay composites

Fig. 9 shows *in vitro* viability of A549 cells treated with 5-FU, 5-FU-MMT hybrid and 5-FU/CS-MMT composites at the different concentrations after 72 h culture incubation. The 5-FU and 5-FU/CS-MMT composites showed similar concentration dependent reduction in cell viability, which was significantly lower than the cells treated only with drug–clay hybrid. These results advocated that 5-FU preserved its antitumor effectiveness even after intercalation of biopolymer in clay.

The *in vitro* therapeutic effect of 5-FU, 5-FU-MMT hybrid and 5-FU/CS-MMT composites can be quantitatively evaluated by IC_{50} at a given time period of cell culture, which is defined as the drug concentration at which 50% cells are killed in given time period. The IC_{50} values of 5-FU, 5-FU-MMT hybrid and 5-FU/CS-MMT composites in A549 cell line were 10.38 μg/ml, 0.34 μg/ml and 11.49 μg/ml, respectively, which were obtained by interpolation of the data shown in Fig. 9. Fig. 9 shows that 5-FU-MMT hybrid had a lower IC_{50} than 5-FU/CS-MMT composites. This is due to lower loading of 5-FU in clay and the formation of clay clumps on cell surface. In contrast, pristine 5-FU and 5-FU/CS-MMT composites showed parallel effect on cell viability after 72 h of incubation.

3.7. In vivo pharmacokinetics (PK)

Fig. 10 shows the *in vivo* pharmacokinetics, i.e., the plasma drug concentration with respect to time after a single oral administration of pristine drug and drug intercalated in clay and biopolymer/clay composites to male wistar rats at the same concentration of 5-FU (50 mg/kg) ($n = 6$). The key PK parameters were analyzed, and the results are listed in Table 2, which include C_{max} (in ng/ml) and T_{max} (h) – the maximum drug concentration encountered after the drug administration and the time at which C_{max} is reached, MRT (h) – the mean residence time of the drug in the plasma and $AUC_{0-\infty}$ (ng h/ml) – the total area under the curve that represents the *in vivo* therapeutic effects of drug. A few significant advantages of the clay and biopolymer could be concluded from PK data. The pristine 5-FU oral administration caused extremely high peak value of the drug concentration (C_{max}) (~2800 ng/ml), which is much higher than the highest tolerance level of the drug concentration in the plasma and thus would cause serious side effects. Instead, C_{max} for oral administration of the 5-FU-MMT and 5-FU/CS-MMT both located in the therapeutic window. When drug was captured inside the gallery of clay and biopolymer/clay composites prior to oral administration to rats, higher drug concentrations were detected in plasma up to ~48 h with composites. Upon comparing the MRT of pristine 5-FU, it was observed that the 5-FU-MMT and 5-FU/CS-MMT increased the residence time of the drug in the plasma by ~37 h and ~28 h, respectively. The 5-FU-MMT and 5-FU/CS-MMT significantly reduced $AUC_{0-\infty}$ values and C_{max} values of drug released while improving MRT of drug in plasma which might be responsible for reduced drug toxicity as compared to 5-FU. Thus, the oral administration of 5-FU by loading into the clay and biopolymer/clay composites leads to significant reduction in toxicity.

3.8. In vivo tissue drug distribution, toxicity and histopathological assessment

Fig. 11 shows the distribution of the drug in different tissue/organ at three time intervals after a single oral administration of pristine drug, drug–clay hybrid and drug–biopolymer/clay to male wistar rats at concentration of 5-FU (50 mg/kg). The pure drug distribution in organs followed the order spleen (12 h) > heart (3 h) > testis (12 h) > kidney (3 h) > liver (3 h) > lung (1 h) after oral administration (Fig. 11a). In contrast, the highest concentration of drug–clay hybrid was found in kidney (12 h), followed by liver (12 h) > heart (3 h) > spleen (12 h) > testis (12 h) > lung (1 h) after oral administration (Fig. 11b). The drug distribution with drug/biopolymer–clay composites compared to pure drug, and clay hybrid

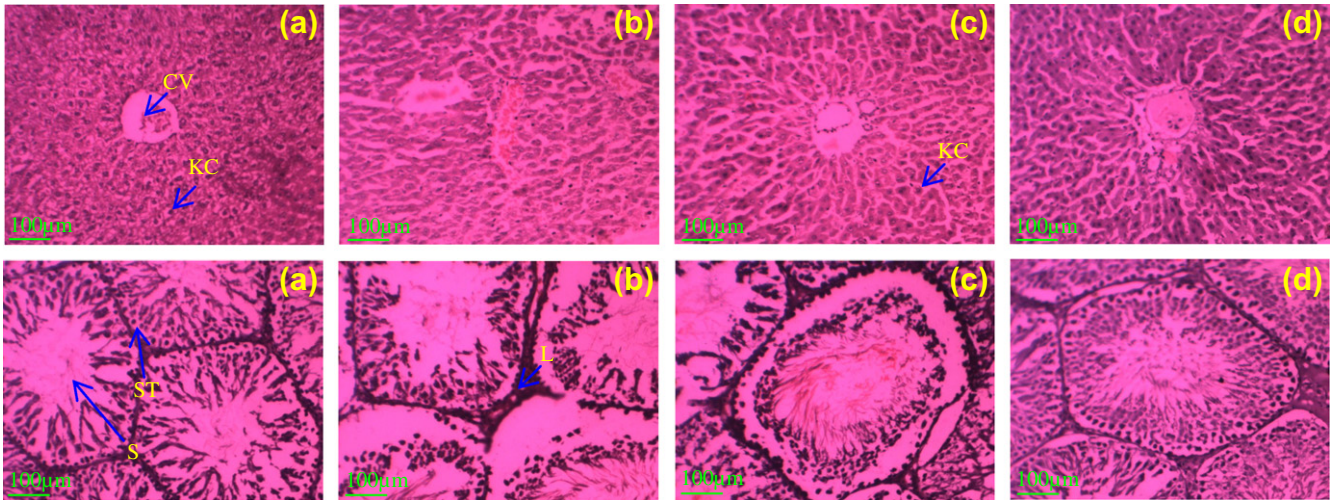

Fig. 13. Histological sections of liver (series I) and testis (series II) samples of male wistar rats were collected at 12 h following a single oral administration of: (a) Normal (b) 5-FU (c) 5-FU-MMT hybrid (d) 5-FU/CS-MMT (*in series I*: *where*, CV: central vein, KC: kupffer cell and *in series II*: *where*, ST: seminiferous tubule, S: maturing sperm, L: leydig cells). (For the interpretation of the references to color in this figure legend, the reader is referred to the web version of this article.)

is presented (Fig. 11c).The maximum drug was found in spleen, and other tissues followed the order liver > heart > testis in 12 h and the least drug concentrations were found in kidney and lung in 3 h. There was significant variation in concentration and time of distribution between pristine drug and drug–clay hybrid/composites in the organs up to 12 h after administration of a single oral dose. It was clearly observed that the drug was released from clay and composites in a controlled manner with the effective distribution in the various active tissues of the rat. Drug–clay hybrid and composites showed a marked reduction in hepatoxicity with time as compared to free drug. SGPT (ALT) and SGOT (AST) levels in plasma were elevated in case of hepatotoxicity. As observed in Fig. 12a and b, the levels of these markers increased significantly in the case of free drug given orally, while in case of the drug formulated in clay and biopolymer, the level of markers reduced with time. Conventional histopathological assessments were carried out to determine the possibility of free drug induced liver and reproductive (testis) toxicity in rats when treated with 5-FU-MMT and 5-FU/CS-MMT. In control group, liver sections, normal hepatic cells (HC), central vein (CV) and kupffer cell (KC) were blurred observed due to staining (Fig. 13 series-Ia). Fig. 13 series-Ib shows the liver sections of rats treated with free drug orally. The liver section was shown ambiguous pathological symptoms in hepatic cells and vein systems. Liver sections of rats treated with oral 5-FU-MMT and 5-FU/CS-MMT were showed relatively less pathological symptoms as compared to free drug (Fig. 13 series-Ic and d). The testicular histology of the normal rat was apparently showed seminiferous tubules (ST), maturing sperm (S) and leydig cells (L) (Fig. 13 series-IIa and d). In contrast, free drug and 5-FU-MMT treated group showed damaged somniferous tubules and cracks in basement membrane (Fig. 13 series-IIb and c).

4. Conclusions

Intercalation of the cationic biopolymer chitosan into Na^+-montmorillonite via cationic exchange process provides composites as drug carriers. *In vitro* release study showed the release of drug from clay/composites by partial diffusion through a swollen matrix/de-intercalation of layers of carriers to its individual components or nanostructures of different compositions. The genotoxicity evaluation of drug in lymphocyte cell culture by comet assay indicated significant retardation in DNA damage when drug was compounded in clay hybrids or composites. *In vitro* cell viability assay showed that the drug efficacy toward cancer cells remained unchanged after incorporation in layered inorganic nanocomposites. *In vivo* pharmacokinetics and biodistribution of formulated drug level in plasma/tissues were within therapeutic window as compared to free drug. The liver toxicity markers indicated a significant reduction in hepatotoxicity when drug was compounded in clay and composites. The liver/testicular histological results also indicated reduced pathological symptoms of drug when administered as composites. Were these results indicated that clay has excellent prospective as a drug carrier for the treatment for cancer with reduced side effects.

Acknowledgments

Authors are thankful to Directors, CSMCRI, Bhavnagar, Institute of Science, Nirma University and Department of Zoology, Gujarat University, Ahmedabad, for providing necessary infrastructure facilities and the Council of Scientific and Industrial Research (CSIR), Government of India, New Delhi, India, for financial support. Authors are also thankful for helping and co-operation rendered by Dr. P. Bhatt (XRD), Mr. V. Agarwal (FT-IR) and Mrs. Sheetal Patel (TGA) of the analytical section of the CSMCRI.

Appendix A. Supplementary material

Supplementary data associated with this article can be found, in the online version, at doi:10.1016/j.ejpb.2012.01.004.

References

[1] S.N. Gupta, N. Aggarwal, A gastro-retentive floating delivery system for 5-fluorouracil, Asian J. Pharm. Sci. 2 (2007) 143–149.
[2] M.S. Lesniak, H. Brem, Targeted therapy for brain tumours, Nat. Rev. Drug Discov. 3 (2004) 499–508.
[3] B. Arıca, S. Calıs, H.S. Kas, M.F. Sargon, A.A. Hıncal, 5-Fluorouracil encapsulated alginate beads for the treatment of breast cancer, Int. J. Pharm. 242 (2002) 267–269.
[4] F. Qian, N. Nasongkla, J. Gao, Membrane-encased polymer millirods for sustained release of 5-fluorouracil, J. Biomed. Mater. Res. 61 (2002) 203–211.
[5] V.S. Shenoy, R.P. Gude, R.S. Ramachandra Murthy, *In vitro* anticancer evaluation of 5-fluorouracil lipid nanoparticles using B16F10 melanoma cell Lines, Int. Nano Lett. 2 (2012) 14–24.

[6] D. Elias, T. de Baere, L. Sideris, M. Ducreux, Regional chemotherapeutic techniques for liver tumors: current knowledge and future directions, Surg. Clin. North Am. 84 (2004) 607–625.
[7] Y. Wang, C. Gong, L. Yang, Q. Wu, S. Shi, H. Shi, Z. Qian, Y. Wei, 5-FU-hydrogel inhibits colorectal peritoneal carcinomatosis and tumor growth in mice, BMC Cancer 10 (2010) 402.
[8] P. Kalantarian, A.R. Najafabadi, I. Haririan, A. Vatanara, Y. Yamini, M. Darabi, K. Gilani, Preparation of 5-fluorouracil nanoparticles by supercritical antisolvents for pulmonary delivery, Int. J. Nanomed. 5 (2010) 763–770.
[9] I. Jungkyun, B. Goutam, K. Wanil, K. Kyong-Tai, Sung-Kee Chung, A blood-brain barrier permeable derivative of 5-fluorouracil: preparation, intracellular localization, and mouse tissue distribution, Bull. Korean Chem. Soc. 32 (2011) 873–879.
[10] D.B. Longley, D.P. Harkin, P.G. Johnston, 5-Fluorouracil: mechanisms of action and clinical strategies, Nat. Rev. Cancer 3 (2003) 330–338.
[11] P. Noordhuis, U. Holwerda, C.L. Van der Wilt, C.J. Van Groeningen, K. Smid, S. Meijer, H.M. Pinedo, G.J. Peters, 5-Fluorouracil incorporation into RNA and DNA in relation to thymidylate synthase inhibition of human colorectal cancers, Ann. Oncol. 15 (2004) 1025–1032.
[12] N.H. Nicolay, D.P. Berry, R.A. Sharma, Liver metastases from colorectal cancer: radioembolization with systemic therapy, Nat. Rev. Clin. Oncol. 6 (2009) 687–697.
[13] R.B. Diasio, Z. Lu, Dihydropyrimidine dehydrogenase activity and fluorouracil chemotherapy, J. Clin. Oncol. 12 (11) (1994) 2239–2242.
[14] E.C. Gamelin, E.M. Danquechin-Dorval, Y.F. Dumesnil, P.J. Maillart, M.J. Goudier, P.C. Burtin, et al., Relationship between 5-fluorouracil (5-FU) dose intensity and therapeutic response in patients with advanced colorectal cancer receiving infusional therapy containing 5-FU, Cancer 77 (3) (1996) 441–451.
[15] E. Aranda, E. Diaz-Rubio, A. Cervantes, A. Anton-Torres, A. Carrato, T. Massuti, et al., Randomized trial comparing monthly low-dose leucovorin and fluorouracil bolus with weekly high-dose 48-hour continuous-infusion fluorouracil for advanced colorectal cancer: a Spanish Cooperative Group for Gastrointestinal Tumor Therapy (TTD) study, Ann. Oncol. 9 (7) (1998) 727–731.
[16] R.L. Schilsky, J. Hohneker, M.J. Ratain, L. Janisch, L. Smetzer, V.S. Lucas, et al., 3rd Phase I clinical and pharmacologic study of eniluracil plus fluorouracil in patients with advanced cancer, J. Clin. Oncol. 16 (4) (1998) 1450–1457.
[17] S. Li, A. Wang, W. Jiang, Z. Guan, Pharmacokinetic characteristics and anticancer effects of 5-fluorouracil loaded nanoparticles, BMC Cancer 8 (103) (2008) 1–9.
[18] B.D. Kevadiya, G.V. Joshi, H.C. Bajaj, Layered bionanocomposites as carrier for procainamide, Int. J. Pharm. 388 (2010) 280–286.
[19] Y. Dong, S.S. Feng, Poly (D,L-lactide-co-glycolide)/montmorillonite nanoparticles for oral delivery of anticancer drugs, Biomaterials 26 (2005) 6068–6076.
[20] S.S. Feng, L. Mei, P. Anitha, C.W. Gan, W. Zhou, Poly(lactide)-vitamin E derivative/montmorillonite nanoparticle formulations for the oral delivery of docetaxel, Biomaterials 30 (2009) 3206–3297.
[21] F.H. Lin, Y.H. Lee, C.H. Jian, J.M. Wong, M.J. Shieh, C.Y. Wang, A study of purified montmorillonite intercalated with 5-fluorouracil as drug carrier, Biomaterials 23 (2002) 1981–1987.
[22] R.W. Korsmeyer, R. Gurny, E. Doelker, P. Buri, N.A. Peppas, Mechanisms of solute release from porous hydrophilic polymers. Int. J. Pharm. 15 (1983) 25–35.
[23] D.A. Hungerford, Leukocytes cultured from small inoculum of whole blood and the preparation of chromosomes by treatment with hypotonic KCI, Stain. Technol. 40 (1965) 333–338.
[24] N.P. Singh, M.T. McCoy, R.R. Tice, E.L. Schneider, A simple technique for quantitation of low levels of damage in individual cells, Exp. Cell Res. 175 (1988) 184–191.
[25] E.E. Visvardis, A.M. Tassiou, S.M. Piperakis, Study of DNA damage induction and repair capacity of fresh and cryopreserved lymphocytes, exposed to H_2O_2 and γ-irradiation, with the alkaline comet assay, Mut. Res. 383 (1997) 71–80.
[26] Z. Rahman, K. Kohli, S.Q. Zhang, R.K. Khar, M. Ali, N.A. Charoo, et al., In-vivo evaluation in rats of colon-specific microspheres containing 5-fluorouracil, J. Pharm. Pharm. 60 (2008) 615–623.
[27] M. Darder, M. Colilla, E. Ruiz-Hitzky, Biopolymer–clay nanocomposites based on chitosan intercalated in montmorillonite, Chem. Mater. 15 (2003) 3774–3780.
[28] Y. Shchipunov, N. Ivanova, V. Silantev, Bionanocomposites formed by in situ charged chitosan with clay, Green Chem. 11 (2009) 1758–1761.
[29] M. Kondo, M. Araie, Iontophoresis of 5-fluorourocil into the conjunctiva and sclera, Invest. Ophthal. Vis. Sci. 30 (3) (1989) 583–585.
[30] B.N. Singh, R.B. Singh, J. Singh, Effects of ionization and penetration enhancers on the transdermal delivery of 5-fluorouracil through excised human stratum corneum, Int. J. Pharm. 298 (2005) 98–107.
[31] G.V. Joshi, B.D. Kevadiya, H.A. Patel, H.C. Bajaj, R.V. Jasra, Montmorillonite as a drug delivery system: intercalation and *in vitro* release of timolol maleate, Int. J. Pharm. 374 (2009) 53–57.
[32] Q. Yuan, J. Shah, S. Hein, R.D.K. Misra, Controlled and extended drug release behavior of chitosan-based nanoparticle carrier, Acta Biomater. 6 (2010) 1140–1148.